Partial oxidation of methane over ruthenium catalysts

Michel G. Poirier, Josée Trudel

Laboratoire de Recherche en Diversification Energétique, CANMET, EMR Canada, 1615 Montée Ste-Julie, PO Box 4800, Varennes, Quebec, Canada J3X 1S6

and

Daniel Guay

Institut National de la Recherche Scientifique-Energie et Matériaux, 1650 Montée Ste-Julie, PO Box 1020, Varennes, Quebec, Canada J3X 1S2

Received 16 March 1993; accepted 19 June 1993

The catalytic partial oxidation of methane with oxygen to produce synthesis gas was studied under a wide range of conditions over supported ruthenium catalysts. The microreactor results demonstrated the high activity of ruthenium catalysts for this reaction. A catalyst having as little as 0.015% (w/w) Ru on Al_2O_3 gave a higher synthesis gas selectivity than a catalyst having 5% Ni on SiO_2. XANES measurements for fresh and used catalyst samples confirmed that ruthenium is reduced from ruthenium dioxide to ruthenium metal early during the experiments. Ruthenium metal is thus the active element for the methane partial oxidation reaction.

Keywords: Methane partial oxidation; synthesis gas; XANES; Ru/Al_2O_3 catalysts

1. Introduction

Hydrogen and synthesis gas, a mixture of carbon monoxide and hydrogen, are mainly produced by the steam reforming of light hydrocarbons, natural gas being generally the feedstock of choice. An alternative process is the partial oxidation of hydrocarbons using molecular oxygen. For methane, the major constituent of natural gas, the two reactions are

$$CH_4 + H_2O \rightleftharpoons CO + 3H_2$$

$$\Delta_r H^\circ_{1000K} = 225.4\,\text{kJ mol}^{-1} \quad \text{(steam reforming)}, \tag{1}$$

$$CH_4 + \tfrac{1}{2}O_2 \rightarrow CO + 2H_2$$

$$\Delta_r H^\circ_{1000K} = -22.2\,\text{kJ mol}^{-1} \quad \text{(partial oxidation)}. \tag{2}$$

The main advantage of the partial oxidation reaction over steam reforming is that

it is slightly exothermic instead of being strongly endothermic. The advantages of the steam reforming reaction include the fact that there is no need for pure oxygen, or nitrogen separation if air is used as the oxidant, and that the amount of hydrogen produced per unit of methane is 50% higher. These advantages have made steam reforming the process of choice for the industry for economic reasons, but for the production of small volumes of hydrogen, partial oxidation may be cheaper.

The catalytic partial oxidation of methane has been studied in the past [1–3] and again recently [4–12]. In the 1940's, Prettre et al. [2] studied the reaction over a nickel catalyst and concluded that synthesis gas is produced by a complex mechanism where the methane/oxygen mixture reacts first following exothermic reactions, to give mainly water and CO_2. In a second step, water and CO_2 rapidly react further with unconverted methane to give synthesis gas according to reactions (1) and (3),

$$CH_4 + CO_2 \rightleftharpoons 2CO + 2H_2 \quad \Delta_r H^\circ_{1000K} = 260.5\,\mathrm{kJ\,mol^{-1}}. \tag{3}$$

Reactions (1) and (3) are linked through the water gas shift reaction (WGSR),

$$CO + H_2O \rightleftharpoons CO_2 + H_2 \quad \Delta_r H^\circ_{1000K} = -34.7\,\mathrm{kJ\,mol^{-1}}. \tag{4}$$

The endothermic reactions (1) and (3) use the heat generated by the initial exothermic reactions.

Methane partial oxidation to synthesis gas is thus a two-step process (combustion followed by reforming). The catalysts used must, therefore, be active (i) for methane combustion to CO_2 and water, and (ii) for methane steam reforming and CO_2 reforming to synthesis gas. It is known from methane combustion studies that precious metals like ruthenium are better catalysts than nickel for the methane combustion reactions [13]. It is also known from the work of Kikuchi et al. [14] that the activity of several metals for methane steam reforming follows the relative order: Ru ≈ Rh > Ni > Ir > Pd ≈ Pt >> Co ≈ Fe for 5 wt% metal loading on silica gel. Moreover, stability tests for ruthenium, rhodium and nickel catalysts showed that the first two are stable, whereas the last one loses its activity with time on stream. Following these considerations, ruthenium should prove to be a good catalyst for the partial oxidation of methane.

Recently, the catalytic partial oxidation of methane using oxygen was tested over ruthenium catalysts [4,10,15]. This metal is a lot less expensive than other precious metals which have been tested for the same reaction [4,7,8,10,11]. However, the ruthenium catalysts tested so far were mainly of the pyrochlore structure ($Ln_2Ru_2O_7$, where Ln is a rare earth), and very few results have been obtained with low ruthenium content catalysts. Moreover, in the studies where low ruthenium content catalysts are tested [4,10], the catalytic activity was determined at a fixed temperature and flow rate, and no attempt whatsoever was made to characterize the chemical state of the ruthenium. The present paper reports the high activity of a series of catalysts made of small amount of ruthenium supported on γ-Al_2O_3. The

catalytic activity toward synthesis gas has been determined at increasing temperature and at various flow rates. The ruthenium oxidation state for the as-prepared and the used catalysts has been determined from XANES measurements. Finally, the activities of these low content ruthenium catalysts are compared with the activities of nickel catalysts.

2. Experimental

2.1. CATALYST PREPARATION

Batches of the different supported ruthenium catalysts were prepared by dissolving $RuCl_3 \cdot 3H_2O$, 99.9% (Johnson Matthey – AESAR Group, #11043, 99.9% purity) in demineralized water, and by adding γ-Al_2O_3 (Aldrich, #19,997-4, 150 mesh, 155 m^2/g) to the solution. The resulting suspension was stirred and evaporated to dryness over a heating plate. The solid obtained was placed in an oven at 105°C for 16 h. The dry solid was then placed in a quartz reactor located in a furnace and was reduced in flowing hydrogen (100 ml/min) at 2°C/min from ambient temperature to 420°C, with a holding time of 2 h at 420°C. The temperature was then lowered, hydrogen was replaced by oxygen and the catalyst was heated again at 5°C/min from ambient temperature to 600°C, and held at that temperature 20 min. Finally, the catalyst was cooled, weighed, and stored. Four catalysts with different nominal ruthenium loading were prepared: 0.015% (w/w) Ru/Al_2O_3, 0.029% (w/w) Ru/Al_2O_3, 0.1% (w/w) Ru/Al_2O_3,and 1% (w/w) Ru/Al_2O_3.

Two supported nickel catalysts were also prepared: 1% (w/w) Ni/Al_2O_3, and 5% (w/w) Ni/SiO_2. Both were prepared by dissolving $Ni(NO_3)_2 \cdot 6H_2O$ in demineralized water and adding the solid support to the solution. For 1% Ni/Al_2O_3, the γ-Al_2O_3 used was the same as for the ruthenium catalysts. The preparation steps were also the same as for the ruthenium catalysts, except that the maximum temperature for the reduction was 450°C, which was held for 18 h. The catalyst was then cooled to room temperature and reacted with a mixture of 0.5% oxygen in nitrogen at room temperature for 20 min. For 5% Ni/SiO_2, the support was silica gel (Aldrich, grade 923, 100–200 mesh). The mixture of dissolved $Ni(NO_3)_2 \cdot 6H_2O$ and SiO_2 was evaporated and the solid obtained dried overnight at 105°C. The next day, the solid was calcined in air at 500°C for 4 h. It was then cooled, weighed, and stored.

2.2. CATALYST TESTING

The catalysts were tested in a fixed-bed microreactor. The gases used were monitored by mass flow controllers (MKS Instruments Canada, Ltd.), mixed and directed to a quartz reactor (i.d. = 7 mm). The catalysts were held in the middle of the reactor by a small amount of quartz wool. The thermocouple used by the tempera-

ture controller was inserted in a quartz well, with the tip located inside the catalytic bed. At the exit of the reactor, the gases were analyzed on line, in parallel, with a gas chromatograph (Hewlett-Packard, model 5890A modified by WASSON-ECE Instrumentation) and with a mass spectrometer (Fisons Instruments, VG model 8-80). The gas line between the microreactor and the gas chromatograph was heated above 120°C, and each gas, including water vapor, was analyzed once every 18 min. A cold trap maintained below 0°C was used along the line between the microreactor and the mass spectrometer, thus allowing the rapid analysis of every gas except water. About 200 mg of catalyst was used for each experiment. The gases used were oxygen (Linde, extra dry grade), methane (Linde, UHP grade) and helium (Linde, UHP grade). The latter was added as a diluent. The $CH_4/O_2/He$ ratio was 8/4/3 for all the experiments. The methane + oxygen flow rate was varied between 90 and 450 ml NTP per minute (methane flow rate between 0.223 to 1.116 mol(CH_4) kg^{-1} s^{-1}). For the experiments at different flow rates, the temperature was set at 800°C, and the flow rates were varied randomly, each one being kept for 1 h. All the experiments were performed at a total pressure of 130 ± 7 kPa.

2.3. X-RAY ABSORPTION SPECTROSCOPY

X-ray absorption near edge structure (XANES) measurements at the Ru L_{III} ($\sim$ 2832 eV), Ru L_{II} ($\sim$ 2959 eV) and Cl K (2815 eV) edges were performed on ruthenium catalysts and reference compounds. These measurements were done using the double crystal monochromator of the Canadian Synchrotron Radiation Facilities (CSRF) located at the Synchrotron Radiation Center (SRC) at Wisconsin-Madison University. During the time of the experiments, the storage ring was operated at 1 GeV, with a current of 100 mA.

The energy scale was calibrated by using a ruthenium metallic foil. This sample was runned periodically during the course of the experiment. All the absorption spectra were obtained in the total electron yield mode by recording the sample current. The powdered samples were finely crushed before being spread on a conducting tape.

The raw absorption data were processed according to commonly accepted procedures. For each absorption spectrum, a first-order polynomial equation was fitted to the pre-edge region of the spectrum and subtracted from the entire spectrum. All the spectra presented herein were normalized to unity in the region far above the edge jump. The energy position of the strong resonance observed at the Ru L_{III} and Ru L_{II} edges was determined by a curve fitting procedure with a Gaussian-type function.

2.4. NEUTRON ACTIVATION ANALYSIS

The exact ruthenium content of the four ruthenium catalysts was determined

by neutron activation analysis. A 100–200 mg sample of each catalyst was sealed in a polyethylene vial and irradiated for 1 h in the neutron flux of the Ecole Polytechnique de Montréal SLOWPOKE nuclear reactor. After a cooling time of 48 h, the γ-ray spectrum of the samples was measured with a semiconductor detector. The ruthenium concentration was determined from the number of counts in the Ru-103 peak at 497 keV. Since the XANES measurements showed the presence of chlorine on the ruthenium catalysts, the chlorine content was also determined for ruthenium catalysts and for pure alumina. For chlorine, the samples were irradiated 2 min, the cooling time was 1 h and the number of counts were measured for the Cl-38 peak at 1642 keV.

3. Results

3.1. NEUTRON ACTIVATION ANALYSIS RESULTS

The ruthenium and chlorine contents measured by neutron activation analysis are reported in table 1. The measured ruthenium contents are close to the nominal percentages. The chlorine contents are similar for pure Al_2O_3 and for 0.015 and 0.029% ruthenium catalysts, which means that in these cases, chlorine comes from the alumina support. For the 0.1 and 1% Ru/Al_2O_3 catalysts, the chlorine contents are higher, which results from a contribution of chlorine from $RuCl_3$ precursor.

Table 1
XANES and neutron activation analysis results

Sample	Ru energy position [a] (eV)	Ru content [b] (wt%)	Cl content [b] (wt%)
L_{III} edge			
Al_2O_3	–	–	0.179
Ru metal	2830.6	n.d. [c]	–
$RuCl_3 \cdot 3H_2O$	2831.2	n.d.	n.d.
$RuO_2 \cdot 1.4H_2O$	2832.2	n.d.	–
0.015% Ru/Al_2O_3	2832.6	0.0157	0.148
0.029% Ru/Al_2O_3	2832.6	0.031	0.163
0.1% Ru/Al_2O_3	2832.6	0.108	0.29
1% Ru/Al_2O_3	2832.5	0.96	0.92
1% Ru/Al_2O_3 used	2830.6	n.d.	n.d.
L_{II} edge			
Ru metal	2958.7		
$RuCl_3 \cdot 3H_2O$	2959.3		
$RuO_2 \cdot 1.4H_2O$	2960.2		

[a] XANES analysis.
[b] Neutron activation analysis.
[c] n.d.: not determined.

3.2. XANES RESULTS

X-ray photoabsorption by an atom involves the promotion of a core electron to a bound or continuum state. Accordingly, the absorption process reveals information about the electronic structure of the absorbing atom and its local environment. Fig. 1 shows the Ru L_{III} X-ray absorption edge of ruthenium metal, $RuCl_3 \cdot 3H_2O$ and $RuO_2 \cdot 1.4H_2O$. Each absorption spectrum displays a strong and sharp peak in the vicinity of 2832 eV. This resonance is mainly associated with the promotion of a $2p_{3/2}$ core electron to unfilled or partially filled d orbitals. As observed in table 1, the energy position of this peak varies by as much as 1.6 eV as the formal oxidation state of ruthenium is changed from 0 in ruthenium metal to +4 in ruthenium dioxide. The energy position of this resonance can thus be used as a sensitive probe of the ruthenium oxidation state in a given compound.

At energy above 2832 eV, each spectrum shows a series of rather broad peaks. This part of the spectrum involves the promotion of a $2p_{3/2}$ core electron to continuum states. Due to the very large mean free path of a low-energy photoelectron, multiple-scattering effects are important in that region of the spectrum. As observed in fig. 1, each compound displays a series of very characteristic peaks in that region. Unfortunately, and unlike the case of extended X-ray absorption fine structure (EXAFS) spectroscopy, a definitive model of the phenomenon occurring in that part of the spectrum is still lacking. This part of the spectrum will therefore be used as a fingerprint of the chemical and structural environment of the ruthenium atom in a particular compound.

In the case of $RuCl_3 \cdot 3H_2O$, two other peaks are observed at 2811.7 and 2820.8 eV. They are assigned to the K edge of the chlorine atom which is just below

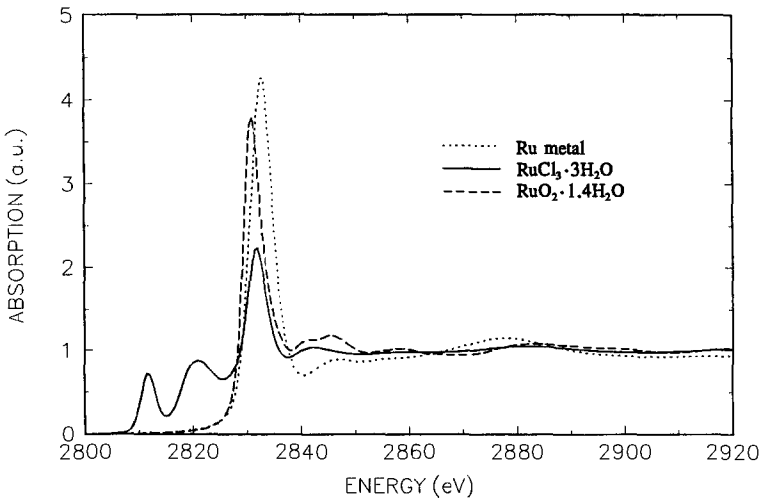

Fig. 1. XANES spectra for reference compounds.

the Ru L_{III} edge. When two absorption edges are so closely spaced, there exists always the possibility that the resonance of one edge interferes with that of the other. In order to check this point, the Ru L_{II} edges of the ruthenium compounds have also been measured. The Ru L_{II} absorption edge occurs at around 2959 eV, well above the Cl K edge. The Ru L_{II} X-ray absorption edge of ruthenium metal, $RuO_2 \cdot 1.4H_2O$ and $RuCl_3 \cdot 3H_2O$ have been measured and found to be very similar to that of their respective parent L_{III} edge. This is not surprising since X-ray photoabsorption at the Ru L_{II} edge involves the promotion of a Ru $2p_{1/2}$ core electron to the same set of bound and continuum states as that involved at the L_{III} edge. More important for our purpose, table 1 shows that, at the Ru L_{II} edge, the correlation between the energy position of the strong resonance and the formal oxidation state of the ruthenium atom is similar to that found previously at the Ru L_{III} edge. This indicates that, at the Ru L_{III} edge, the proximity of the Cl K edge has no effect on the energy position of the resonance that will be used to track the variation of the oxidation state of the ruthenium atom that occurs in the catalyst.

Four different as-prepared ruthenium catalysts have been characterized by X-ray absorption spectroscopy at the Ru L_{III} edge. The energy position of the strong resonance observed in these spectra are listed in table 1. The energy position of this peak is characteristic of a ruthenium atom in a +4 oxidation state (Ru(IV)). The same conclusion is also reached if the structure of the spectrum in the post-edge region is used to identify the chemical environment of the ruthenium, and fig. 2 shows that the L_{III} X-ray absorption edge of the 1% Ru on Al_2O_3 catalyst is similar to that of $RuO_2 \cdot 1.4H_2O$.

The XANES measurements performed on the four catalysts also showed an

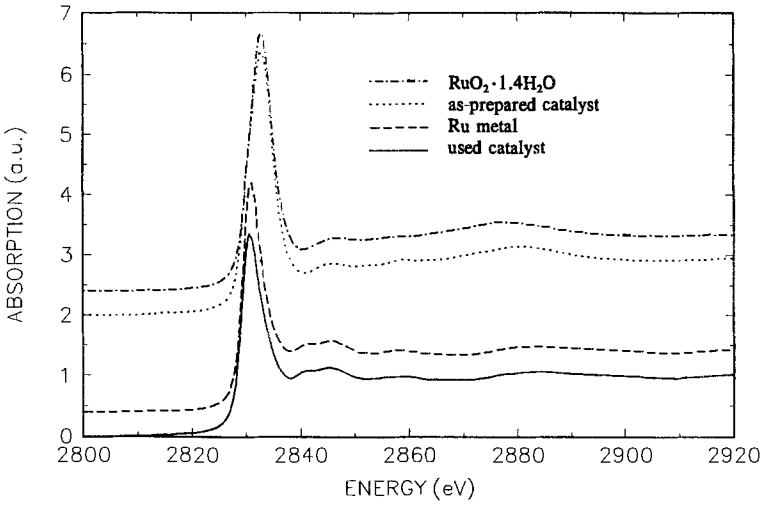

Fig. 2. XANES spectra for as-prepared and used 1% Ru/Al_2O_3 catalyst. (Catalyst tested at 800°C in $CH_4/O_2/He$ ratio of 8/4/3 for 4 h.)

absorption peak associated to the presence of chlorine atoms (this peak is hardly seen in fig. 2). There is little likelihood that a significant fraction of $RuCl_3$ still exist as such after the catalyst preparation procedure used in that study. The thermal decomposition of $RuCl_3$ is routinely used by electrochemists to prepare RuO_2 electrodes and most probably this signal originates from chlorine atom strongly adsorbed on the support itself. This is supported by the fact that the ruthenium L_{II} and L_{III} X-ray absorption edges of the as-prepared catalysts are at the RuO_2 position (Ru(IV)), which excludes a significant contribution from Ru(III) in $RuCl_3$.

It appears that there is a change in the chemical and structural environment of the ruthenium atoms as a result of its use in the reactor. Fig. 2 displays the Ru L_{III} X-ray absorption spectrum of the 1% Ru on Al_2O_3 catalyst after testing. Both the energy position of the strong resonance and the post-edge oscillations correspond to that of ruthenium metal. It appears therefore that, under our experimental conditions, the ruthenium atom is reduced during its use in the reactor to promote the partial oxidation of methane.

3.3. REACTOR RESULTS

A methane/oxygen mixture was reacted over one of the ruthenium catalysts (0.1% Ru/Al_2O_3). The temperature was increased from room temperature to 800°C over 2 h and held for 4 h (see fig. 3). The methane/oxygen reaction started at 425°C, as evidenced by the rapid increase of the catalyst bed temperature (owing to the exothermic reaction) and by the appearance of the product gases H_2, CO,

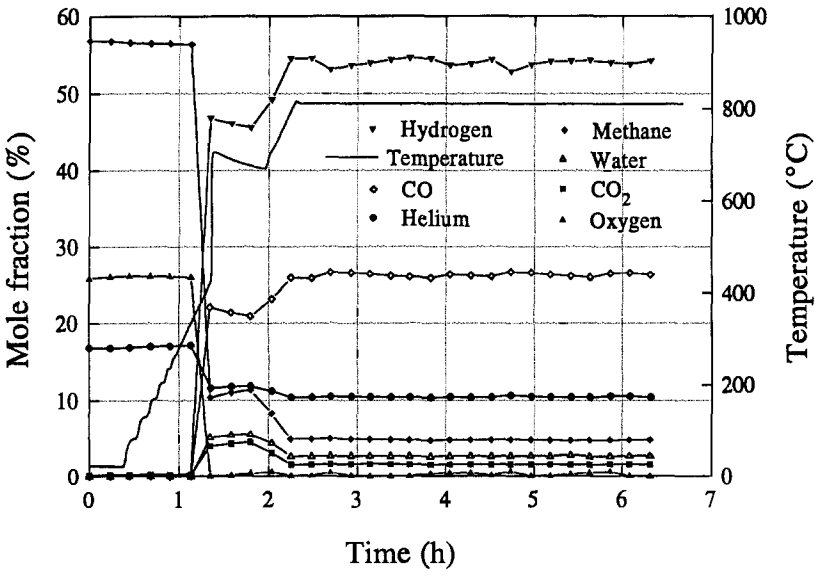

Fig. 3. Activity of a 0.1% Ru/Al_2O_3 catalyst when the temperature is increased from ambient to 800°C, and stability at 800°C. (CH_4/O_2/He ratio of 8/4/3, and methane flow rate of 0.893 mol(CH_4) kg^{-1} s^{-1}.)

CO_2, and H_2O. During the 4 h plateau at 800°C, the catalyst did not show any sign of loss of activity or selectivity.

The activities for the four ruthenium and the two nickel catalysts are reported in table 2. The activities for the methane/oxygen reaction are indicated by the methane conversion ($X_{METHANE}$) and by the oxygen conversion (X_{OXYGEN}). The activities for methane steam reforming (reaction (1)) and for methane CO_2 reforming (reaction (3)) are related to the equilibrium constants calculated from the product gas composition. For a chemical reaction, the thermodynamic equilibrium constant is

$$K = \exp(-\Delta_r G/RT) = \prod_i (p_i)_e^{v_i} = (P_t)_e^{v} \prod_i (y_i)_e^{v_i}, \tag{5}$$

where $\Delta_r G$ is the Gibbs free energy of the reaction at temperature T, R is the universal gas constant (0.008315 kJ mol^{-1} K^{-1}), T is the reaction temperature in K, $(p_i)_e$ is the partial pressure in atm of gas i at equilibrium, $(y_i)_e$ is the mole fraction of gas i at equilibrium, $(P_t)_e$ is the total pressure in atm at equilibrium, and v is the sum of the stoichiometric coefficients ($\sum_i v_i$).

The values of the K's are calculated from the left part of eq. (5) using thermodynamic data ($\Delta_r G$). The activity and selectivity of the catalysts are evaluated using the experimental y_i and P_t, in an equation derived from the right part of eq. (5),

$$\Psi = (P_t)^{v} \prod_i (y_i)^{v_i}, \tag{6}$$

where y_i is the experimental mole fraction of gas i, and P_t is the total pressure in atm in the catalytic reactor.

Eq. (6) has been used for reaction (1) (Ψ_1), reaction (3) (Ψ_3), and reaction (4)

Table 2
Activity of ruthenium and nickel catalysts for the partial oxidation of methane (800°C, CH_4/O_2/He ratio of 8/4/3, methane flow rate of 0.893 mol(CH_4) kg^{-1} s^{-1}) [a]

Sample	$X_{METHANE}$ (%)	X_{OXYGEN} (%)	Ψ_1	Ψ_3	Ψ_4	Activity (mol(CH_4) kg^{-1} s^{-1})
1% Ru/Al_2O_3	88.1	99.2	78.7	65.5	1.200	0.787
0.1% Ru/Al_2O_3	84.7	99.7	51.2	47.3	1.082	0.753
	85.3	100	48.2	39.5	1.220	0.760
0.029% Ru/Al_2O_3	85.5	99.3	42.6	49.1	0.870	0.760
0.015% Ru/Al_2O_3	66.3	99.3	1.84	4.1	0.448	0.592
5% Ni/SiO_2	46.6	85.4	0.228	0.495	0.461	0.416
1% Ni/Al_2O_3	18.7	40.1	5.2×10^{-3}	9.4×10^{-3}	0.556	0.167
Al_2O_3	5.0	13.0	2.1×10^{-5}	3.0×10^{-5}	0.680	0.045
therm. equil. [b]	–	–	≈ 170	≈ 150	1.081	–

[a] $X_{METHANE}$ and X_{OXYGEN} stand for methane conversion and oxygen conversion. Ψ's are defined in the text. Activity is the methane conversion times the methane flow rate (0.893 mol(CH_4 kg^{-1} s^{-1}).

[b] Thermodynamic equilibrium. Calculated from $\Delta_r G$ at 800°C.

(Ψ_4). The total pressure inside the reactor during the experiments was 1.2 atm. For reactions (1) and (3), $\upsilon = 2$, and for reaction (4), $\upsilon = 0$. Results of $X_{METHANE}$, X_{OXYGEN} and Ψ's are shown in table 2. The experiments with 0.1% Ru/Al_2O_3 were repeated two times, and the results reported in table 2 show that there are small differences in Ψ values that are associated with experimental errors. It is seen from those results that the gas composition that is the closest to equilibrium is obtained with the 1% Ru/Al_2O_3 catalyst. When the ruthenium content decreases below 1%, the gas composition moves away from the equilibrium composition. It is remarkable that under our experimental conditions, the catalyst having only 0.015% ruthenium is more active ($X_{METHANE}$, X_{OXYGEN}, Ψ_1 and Ψ_3 higher) than the one with 5% nickel. Finally, the less active catalysts are 1% Ni/Al_2O_3 followed by pure Al_2O_3.

The values of Ψ_1 and Ψ_3 never approached the equilibrium values. For the two most active catalysts, 0.1 and 1% Ru/Al_2O_3, the Ψ_4 values are close to the thermodynamic equilibrium and $\Psi_1 > \Psi_3$. For the other catalysts, Ψ_4 is lower than the thermodynamic equilibrium value and $\Psi_1 < \Psi_3$. This suggests that reaction (1) (steam reforming of methane) is more affected by the catalysts than reaction (3) (CO_2 reforming of methane), and that reaction (4) (WGSR) does not reach equilibrium under our experimental conditions over the less active catalysts.

The high activity of the ruthenium catalysts is further demonstrated by the results of oxygen conversion as a function of methane/oxygen flow rates. This is reported in fig. 4, as the percentage of unconverted oxygen ($1 - X_{OXYGEN}$) over the

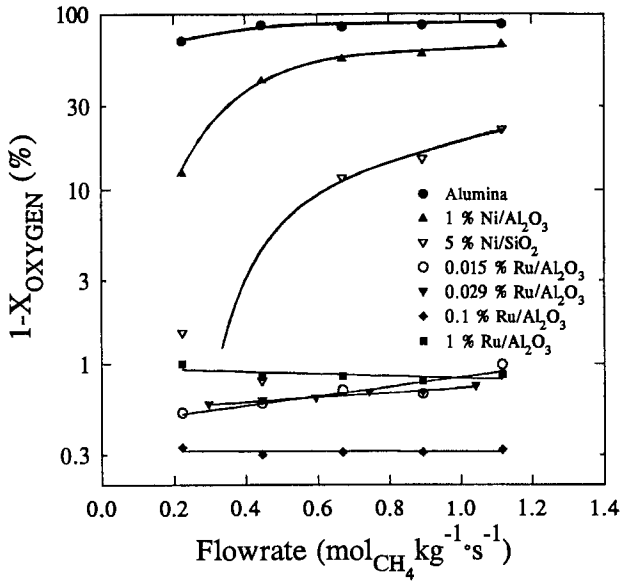

Fig. 4. Non-consumed oxygen during microreactor experiments as a function of methane flow rate for the different catalysts used. (CH_4/O_2/He ratio of 8/4/3, 800°C, 200 mg of catalyst.)

different catalysts at increasing flow rates. Fig. 4 shows that the four ruthenium catalysts have oxygen conversion of 99% or better for the entire flow rate range studied, which clearly shows their high activity for the methane partial oxidation reaction. The two nickel catalysts show decreasing oxygen conversion with an increase in flow rate, the effect being more important from 0.223 to 0.670 mol(CH_4) kg^{-1} s^{-1}. Finally, γ-Al_2O_3 is not active for the methane/oxygen reaction.

4. Discussion and conclusion

For the four ruthenium catalysts examined, we believe that the temperature at which the catalysts start to be active (the lightoff temperature) corresponds to the temperature where the reduction of RuO_2 to ruthenium metal by methane occurs. The XANES measurement performed on the used 1% Ru/Al_2O_3 catalysts confirmed that ruthenium was reduced to the metallic state in the course of the experiment. Moreover, a similar behavior was reported in two papers for methane partial oxidation over $Pr_2Ru_2O_7$ pyrochlore catalyst. First, Ashcroft et al. [4] did XPS analysis on used $Pr_2Ru_2O_7$ catalyst and observed ruthenium metal. Then, Poirier et al. [15] performed TG/DTA analysis over a fresh sample of $Pr_2Ru_2O_7$ and observed that the catalyst was reduced at 420°C to ruthenium metal and Pr_2O_3, and this initiated the methane partial oxidation reaction. As for $Pr_2Ru_2O_7$ structure, the low content ruthenium oxide catalysts underwent a reduction at about 400–500°C. This proved that it is ruthenium metal that is active for the selective production of synthesis gas from methane/oxygen mixtures.

Fig. 3 results show that when the methane/oxygen reaction begins, there is a sharp increase of the catalyst temperature, as recorded by the thermocouple located inside the catalytic bed. The temperature reaches about 700°C, and then decreases slowly with time. When the programmed temperature reaches the catalyst temperature, the temperature increases again up to 800°C. The products gas composition reflects these temperature changes, since higher temperature increases CO and H_2 concentrations. The high flow rate used in this study, combined to the heat generated by the reaction, caused some uncertainties as to the exact temperature. Vermeiren et al. [5] reported a temperature increase of almost 100°C with a methane flow rate of 0.22 mol(CH_4) kg^{-1} s^{-1}. Here, we have tried to minimize the temperature increase by using the thermocouple inside the catalytic bed to control the furnace output. Somewhat lower or higher temperatures may, however, have been encountered in some part of the catalyst bed as the first exothermic reactions mainly occur in the inlet portion of the catalytic bed and the endothermic reforming reactions occur farther. The temperature variations are, however, similar for all the catalysts tested here.

The activities of our 1, 0.1 and 0.029% ruthenium catalysts are high enough to convert all the oxygen present and to produce mainly synthesis gas, at 800°C and at a flow rate of 0.893 mol(CH_4) kg^{-1} s^{-1}, as shown by the Ψ_1 and Ψ_3 values reported

in table 2. With the 0.015% ruthenium catalyst, however, even if oxygen is still completely consumed, the synthesis gas selectivity is lower, which indicates a lower activity. In the literature, the only results previously reported for this reaction with similar catalysts are from Ashcroft et al. [4], who tested 1 and 0.1% Ru/Al_2O_3 catalysts at 777°C with a methane flow rate of 0.089 mol(CH_4) kg^{-1} s^{-1}. Their 1% ruthenium catalyst yielded a high synthesis gas selectivity, but with their 0.1% ruthenium catalyst, the synthesis gas selectivity was significantly lower, which is surprising considering the very low flow rate used in their tests. To ascertain that this difference is not due to a temperature effect, we performed one experiment at 0.179 mol(CH_4) kg^{-1} s^{-1}, with 50 mg of 0.1% Ru/Al_2O_3 catalyst and a CH_4/O_2/He ratio of 8/3/89, and observed at 680°C the complete conversion of oxygen and the selective formation of synthesis gas (near thermodynamic equilibrium).

The higher activity obtained here is not related to the presence of chlorine on the catalysts since there is as much chlorine on pure alumina as in 0.029% ruthenium catalyst, and the activity of pure alumina is very low compared to this ruthenium catalyst. The results obtained with the ruthenium catalysts are also better than those obtained with the two nickel catalysts tested in this work. Other available results for nickel catalysts do not show better activity than our ruthenium catalysts. Results reported by Vermeiren et al. [5] for their 5% Ni/Al_2O_3 catalyst at 800°C are better than those obtained here with nickel catalysts, but are not as good as those obtained with our ruthenium catalysts due to the lower flow rate used by Vermeiren et al. These authors got a maximum activity of 0.527 mol(CH_4) kg^{-1} s^{-1} which compares well to the value of 0.416 mol(CH_4) kg^{-1} s^{-1} shown in table 2 for our 5% nickel catalyst at the same temperature, but is, however, significantly lower than the activity of our ruthenium catalysts (from 0.592 to 0.787 mol(CH_4) kg^{-1} s^{-1}, in table 2). Vernon et al. [10] tested several catalysts, including Ni/Al_2O_3 and 1% Ru/Al_2O_3, and found similar methane conversions and synthesis gas selectivities for these two catalysts. The lower synthesis gas selectivity observed in our experiments with nickel catalysts comes from the higher flow rate (and consequently the lower contact time between the gas and the catalyst) used here, which is 0.893 mol(CH_4) kg^{-1} s^{-1} compared to 0.089 mol(CH_4) kg^{-1} s^{-1} for the experiments of Vernon et al. At this high flow rate, our nickel catalysts cannot bring reactions (1) and (3) as close to the equilibrium values as the ruthenium catalysts do. The other study with nickel catalysts used very low methane flow rate [6]. The higher activity of ruthenium catalysts compared to nickel catalysts is thus obvious because no nickel catalyst has been reported to lead to an activity as high as those reported here for ruthenium catalysts, and because this high activity was obtained with catalysts having 0.1% ruthenium content or less.

The high activity of ruthenium catalysts, combined with their high selectivity for synthesis gas (high activity for reactions (1) and (3)), make them excellent methane partial oxidation catalysts. Moreover, compared to nickel, ruthenium is more stable, does not form volatile carbonyl under experimental conditions as nickel did, is less susceptible to be reoxidized during reaction and does not lead to

carbon deposition. Volatilisation of some ruthenium oxides (RuO_3 and RuO_4) has previously been reported [16] under oxidizing conditions, but that problem was not encountered in our experiments. Finally, the advantages of ruthenium have to be weighed against its major drawback, a cost of about 150 times that of nickel. That drawback may be less important for a small unit than for a large industrial-scale unit.

Acknowledgement

We have benefited from discussions with Gilles Jean and Kim Ah-You, and from laboratory assistance by Martin Chassé. We thank the Canadian Synchrotron Radiation Facilities (CSRF) for dedicated runs at the Synchrotron Radiation Center (SRC) at Wisconsin-Madison University.

References

[1] C. Padovani and P. Franchetti, Giorn. Chem. Ind. Applicata 15 (1933) 429.
[2] M. Prettre, Ch. Eichner and M. Perrin, Trans. Faraday Soc. 43 (1946) 335.
[3] K. Peters, M. Rudolf and H. Voetter, Brennstoff-Chem. 36 (1955) 257.
[4] A.T. Ashcroft, A.K. Cheetham, J.S. Foord, M.L.H. Green, C.P. Grey, A.J. Murrell and P.D.F. Vernon, Nature 344 (1990) 319.
[5] W.J.M. Vermeiren, E. Blomsma and P.A. Jacobs, Catal. Today 13 (1992) 427.
[6] D. Dissanayake, M.P. Rosynek, K.C.C. Kharas and J.H. Lunsford, J. Catal. 132 (1991) 117.
[7] A.K. Bhattacharya, J.A. Breach, S. Chand, D.K. Ghorai, A. Hartridge, J. Keary and K.K. Mallick, Appl. Catal. A 80 (1992) L1.
[8] J.K. Hochmuth, Appl. Catal. B 1 (1992) 89.
[9] V.R. Choudhary, A.M. Rajput and B. Prabhakar, Catal. Lett. 15 (1992) 363.
[10] P.D.F. Vernon, M.L.H. Green, A.K. Cheetham and A.T. Ashcroft, Catal. Lett. 6 (1990) 181.
[11] R.H. Jones, A.T. Ashcroft, D. Waller, A.K. Cheetham and J.M. Thomas, Catal. Lett. 8 (1991) 169.
[12] V.R. Choudhary, S.D. Sansare and A.S. Mamman, Appl. Catal. A 90 (1192) L1–L5.
[13] R. Prasad, L.A. Kennedy and E. Ruckenstein, Catal. Rev.-Sci. Eng. 26 (1984) 1.
[14] E. Kikuchi, S. Tanaka, Y. Yamazaki and Y. Morita, Bull. Japan Petrol. Inst. 16 (1974) 95.
[15] M.G. Poirier, G. Jean and M.P. Poirier, Stud. Surf. Sci. Catal. 73 (1992) 359.
[16] S.J. Tauster, L.L. Murrell and J.P. DeLuca, J. Catal. 48 (1977) 258.